Second and modified-variable order kinetic models of oil shale and kerogen pyrolysis

M. Suleiman[2], M. Harahshah[3] and Omar Al-Ayed[1]*
[1]Al-Balqa Applied University, Faculty of Engineering Technology, Department of Chemical Engineering, Amman 11134 Jordan; E-mail: osalayed@fet.edu.jo

[2] Al-Balqa Applied University, Civil Engineering Department
* On Leave, Middle East University, Amman, Jordan

[3]Al-Husein Ibn Talal University, Department of Mining and Environmental Engineering, Amman, Jordan

Abstract

Kinetics of oil shale and de-mineralized kerogen pyrolysis were determined for Jordanian oil shale using a thermogravimetric analyzer. Kinetic experiments were conducted with heating rates of 1, 3, 5, 10 and 30°C min-1. The activation energies and pre-exponential factors were initially determined using the Coats and Friedman equation for a second order reaction. In this case, the activation energies were found to vary with heating rate. The kinetic data were further analyzed using a variable reaction order model, in which the reaction order was a function of the rate of mass loss. The variable order model led to a significant improvement in the agreement between the model results and the experimental data. Interestingly, the reaction order in the variable-order model was at a minimum when the mass loss rate was greatest.

Key word: Variable reaction order, Kinetics, Oil Shale, Modeling, Pyrolysis

Introduction

Oil shale is defined as a sedimentary rock of various origins containing organic matter that, when heated, transforms into solid coke and liquid and gaseous hydrocarbon compounds. Much work was done on pyrolysis of oil shale and its pyrolysis kinetics by Thermogravimetric Analysis (TGA). Different kinetic models, such as Arrhenius, Coates & Redfern, Horowitz & Metzger, and Ingraham & Marrier *et al.*, were used to analyze thermogravimetery data obtained (1).

Campbell et al. (2) studied the rate of evolution of CH_4, H_2, CO, CO_2, and C_2, C_3 hydrocarbons during pyrolysis of Colorado oil shale at linear heating rates varying from 0.5 to 4.0°Cmin^{-1}. More hydrogen release was reported at lower heating rates. Methane formation and evolution initiated at temperature slightly lower than 350°C and reached a maximum value at 445°C. Rate of methane release increased with a decrease in heating rate. Ethane and ethene (C_2) production increased to a maximum value at 450°C and stopped at slightly higher than 550°C. C_3 (propane and propene) production was found to occur at 450°C and its formation was stopped at 525°C. The oil release profile corresponded closely to those observed for C_1 and C_2.

The decomposition of oil shale involves a large number of reactions in parallel and in series, whilst TGA measures the overall weight loss due to these reactions. A combined study (3) using TGA, Diffuse Reflectance Infrared Fourier Transform Spectroscopy, (DRIFTS), and X-ray Diffraction (XRD) resulted in a better insight into oil shale reactions. TGA provides general information on the overall reaction kinetics rather the individual reactions.

Li and Yue, 2003 (4) studied the pyrolysis kinetics of different Chinese oil shale samples at a constant heating rate of 5°Cmin^{-1}. The TGA data obtained were used to develop a kinetic model that assumed 11 first

order parallel reactions with different activation energies and frequency factors. The calculated fractional conversion of each reaction is a complex function of activation energy. Pyrolysis reactions for pyrolysates of oil shale with low activation energies resulted mainly from the rupture of weak chemical bonds, probably the rupture of weak cross-linked bonds, such as, C-O, C-S bonds (5,6) *etc*. Also, the rupture of branched functional groups in kerogen long molecular structure may also have low activation energy, commensurate with pyrolysis gaseous products such as H_2O, CO_2, H_2S, H_2 and light hydrocarbons.

Medium activation energy values are associated with breakup of the side chains in the β-site of aromatics, decomposition of normal alkane with large molecular weight, Diels-Alder cyclization reactions and the rupture of alicyclic hydrocarbons. These reactions occur at pyrolysis temperatures between 420 – 480^{o}C. On the other hand, pyrolysis reactions with high apparent activation energies include mainly the aromatization of alicyclic compounds, dehydrogenation and combination of aromatic rings, and rupture of heterocyclic compounds.

It is clear from the above discussion that kerogen decomposition to produce shale oil and gases is a continuous process composed of several parallel, series, simultaneous and complex reactions. Because heating rate affects the product distribution of the pyrolysis process, the activation energy must also differ and order of reaction must vary. It is possible that the variation of activation energy is associated with decomposition mechanisms, and consequently it is implicitly embedded in variation of reaction order. On the other hand, some workers (27) advocate that activation energy, frequency factor, and reaction order do not have clear meaning when related to the chemical reactions of oil shale.

Workers such as Thakur and Nattall (7) combined isothermal and non-isothermal thermogravimetry analysis to study thermal decomposition of oil shale. They reported that the decomposition involves two consecutive first order reactions with bitumen as an intermediate. Other researchers used pseudo-first-order overall reaction order in their kinetic analysis (8). Turkish oil shale (9) was studied by TGA at non-isothermal conditions under argon, and first order reaction kinetics were found to fit the kinetic data. Some other Turkish oil shale samples (10) were pyrolysed using thermogravimetric analysis in which reaction orders varied between 1.45 and 1.73 to fit the pyrolysis kinetics.

Qing and co-workers (11) used a first order equation in their kinetic study of Huadian oil shale pyrolysis, as it resulted in the best fit of experimental data. Some investigators (12, 13) modeled the kinetics of Ellajjun oil shale using first order reaction kinetics whereas others (14) found a second order model is more suitable. Solid state reaction, *i.e.* oil shale (15-16) is generally not an elementary reaction, in which the reaction model varies with temperature, and the reaction involves several implicit steps with different activation energies. Spanish oil shale (17) rate of oil shale decomposition was suitably described by an overall first order kinetics.

Several researchers (16, 18) advocated that because oil shale pyrolysis is a complicated process with multiple reaction mechanisms, reaction order, $\boldsymbol{n}$, of the order 1 or 2 in the equation $f(x) = (1 - x)^{\boldsymbol{n}}$ is not suitable to describe the overall pyrolysis reaction. The complex Sestak-Berggren (18) equation for oil shale pyrolysis mechanism suggested investigating the multiple reaction mechanisms involved of the form:

$$f(x) = x^m(1-x)^{\boldsymbol{n}}[-ln(1-x)^p] \qquad [1]$$

Where $m, n, and\ p$ are constants, their derivatives implying the different reaction mechanisms, in which the first term, x^m, represents a diffusion mechanism, the second term in equation [1] describes an interface mechanism and finally, the square bracketed quantity is the actual oil shale decomposition mechanism. x is the

conversion based on the end of run. In the present work, the diffusion mechanism is practically absent in TG experiments because of the fine particle size is used; as a result, m is assumed zero. On the other hand, the combined oil shale decomposition and interface mechanisms are assumed to be of the form:

$$f(x) = (1-x)^n \quad [2]$$

Changing reaction order was thought to be related to changing reaction mechanism (19). Without doubt the oil shale kerogen reaction is a multiple reactions system. Oil shale studies suggest that pyrolysis of oil shale is a complex process involving multiple mechanisms at all stages of product evolution and hydrocarbon generation process. Higher reaction order is a measure of the complexity and multiplicity of the mechanism. Several other researchers (20 -25) have studied the kinetics of oil shale pyrolysis and decompositions and most of these investigators used first order reaction kinetics to model isothermal and non-isothermal kinetic data. Integral and differential methods (13-14) were used to model Ellajjun oil shale pyrolysis.

In this work, a mathematical correlation was developed for predicting reaction order as a variable quantity based on rate of mass loss and heating rate. The developed equation for the reaction order $\boldsymbol{n}$ is used in equation [2] to model the rate of mass loss of oil shale due to decomposition during pyrolysis using the TG/DGA data. The proposed equation was tested for different heating rates.

The rate of mass loss is described by the equation

$$\frac{dx}{dt} = kf(x) \quad [3]$$

$$\frac{dx}{dt} = k_o exp(-E/RT)(1-x)^n \quad [4]$$

$$x = (w_o - w_t)/(w_o - w_f) \quad [5]$$

Where w_o is the initial weight of sample.

w_t : Weight of sample at time, t

w_f : Weight of sample measured at end of run.

The activation energy in equation [4] is determined using the Coats & Redfern (26) procedure.

Experimental procedure

The experiments runs were conducted in a Q 500 Thermo-Gravimetric Analyzer. The Q 500 temperature range is ambient to 1000°C, with 1.0 g weighing balance capacity and 0.1 µg sensitivity. The TGA isothermal temperature precision is 0.1 °C and 0.1 – 100 °Cmin^{-1} heating rate range. Nitrogen gas carrier, at a flow rate of 100 cm^{3}min^{-1} was used. The selected size fraction of raw oil shale was 100 - 210µm to avoid mass and/or heat transfer effect on the pyrolysis process. The sample was placed in a desiccator overnight to remove moisture before the pyrolysis study.

About 17 - 20 mg of sample was used in runs. The air in the pyrolysis unit was flushed with nitrogen before performing the analysis. Heating rates of 1, 3, 5, 10, and 30°Cmin^{-1} were used in this study. Each sample was heated to a temperature of 550°C and the weight loss vs. temperature was recorded for each of the five heating rates. Three runs were repeated for each heating rate with relative standard deviation of less that 5%. The average values of TGA curves are reported.

Results and discussion

Data obtained by DGA were used to predict the activation energy according to procedure of Coats and Redfern (26). The mathematical manipulation discussed in earlier works (14) was employed to estimate the activation energy. In these analyses, a plot of the quantity $ln(x/(T^2(1-x))$ against inverse of pyrolysis temperature would result in an estimate of the activation energy. The determination of activation energies at different heating rates was performed under the assumption of second order reaction kinetics. The obtained activation energies and frequency factors according to the Coats & Redfern procedure

Table I: Activation Energy and corresponding pre-exponential values at different heating rates.

Heating rate, ***h*** °C/min	Activation Energy **E** kJ/mol	Pre-exponential factor $\mathbf{k_o}$
1	99	6.8E+6
3	102	2.7E+7
5	114	5.0E+8
10	125	3.2E+9
30	141	1.7E+11

are given in Table I. As reported there, the activation energy increased with increasing heating rate. Estimated values of activation energies were found to be within the range 99 – 141 kJ/mol. These values indicated that heating rate had an impact or influenced the activation energy estimation.

Generally, the reaction was assumed to be either first or second order in most reported oil shale pyrolysis kinetic studies. In this research paper, a novel procedure was deduced to estimate reaction order. The following form of equation was used for reaction order calculations:

$$n = 2exp\left(-R\frac{1}{h}(dw/dt)\right) \qquad [6]$$

Where:

R - Universal Gas Constant, 8.314 J (mol K)$^{-1}$

dw/dt - rate of mass loss, mgmin^{-1} reported during the experiment

x - conversion of oil shale based on total mass loss at 550°C, equation [5].

h - heating rate, in °Cmin^{-1}.

In an attempt to develop a relationship between rate of mass loss and reaction order after the activation energy determination step, it was decided to force fit a reaction order value to the rate of mass loss equation [4], to exactly match with experimental results by adjusting the n value for each individual experimental point. The outcome of such an attempt is the generation of a set of scattered values of variable reaction order with rate of mass loss. Furthermore, the rate of mass loss values were plotted against these adjusted (force fitted) scattered values of reaction order as indicated in Figure 1 to obtain the following empirical equation.

$$n = 1.996exp\left(-8.14(dw/dt)\right) \qquad [7]$$

Equation [7] when applied to pyrolysis kinetics data improved the fit of rate of mass loss data to some extent. The predicted values of rate of mass loss according to generated orders using the equation [7] were higher in magnitude than experimental data points, as a result; equation [7] was further modified by dividing the exponential quantity by heating rate to be in its final form as indicated by equation [6].

The experimental rate of mass loss showed a maximum value with pyrolysis temperature. This trend was observed for all runs but with a decrease in magnitude as heating rate was decreased. The increase in rate of mass loss and its associated occurrence temperature is apparently ascribed to increase in heating rate where heating flux was higher and may also include the contribution of any inherent catalytic activity of the mineral material of oil shale, in the absence of diffusion effects.

The rate of mass loss according to equation [4] was obtained for the second order assumption and for the suggested variable order as expressed by equation [6]. The activation energy used in equation [4] was the estimated values according to the Coats & Redfern procedure.

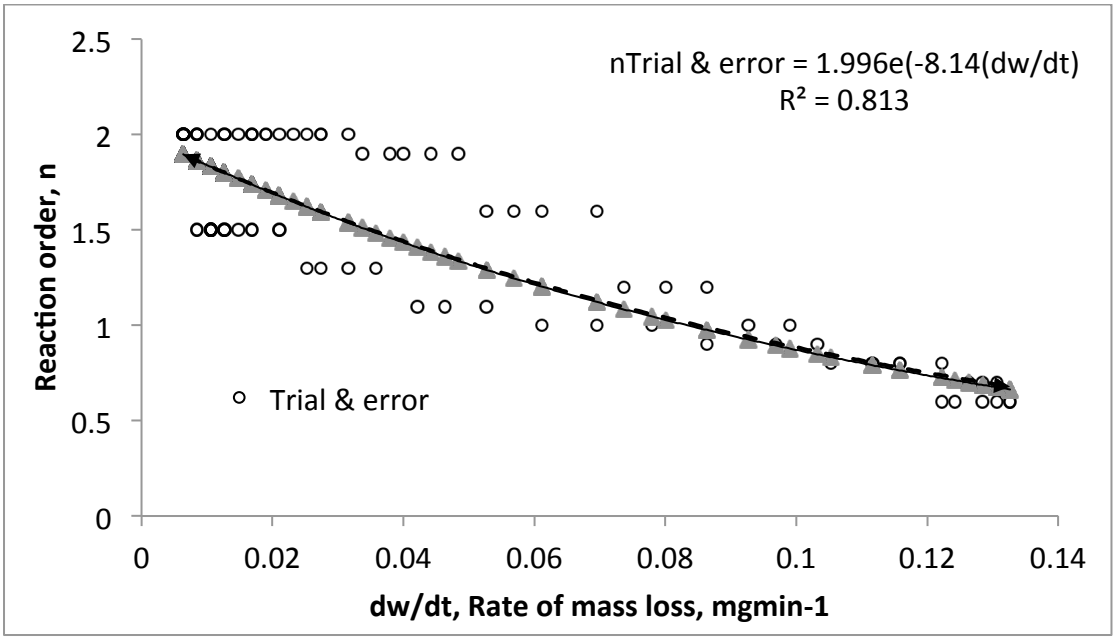

Figure 1: Reaction order and rate of mass loss for variable order determination

The variable reaction order as expressed by equation [6] was interpreted to be a function of the universal gas constant, **R**, rate of mass loss (mg/min) and heating rate (^{o}C/min). The numerical values of the reaction order varied between 1.9 and 1.4. Similar ranges of values were also reported and used [10] to model pyrolysis kinetics of Turkish oil shale. The highest value of variable reaction order calculated from initial rates of mass loss where initial decomposition of oil shale was low and at various heating rates in all experimental runs was close to 1.9. The minimum value of reaction order was observed at the highest mass loss rate. The estimated values of reaction order increased with a decrease in rate of mass loss after the highest rate of mass loss was observed.

This trend was quite clear from the nature of the curve convexity of the rate of mass loss with pyrolysis temperature. The developed equation for reaction order indicated an inverse proportionality with rate of mass loss. The minimum value of reaction order found was approximately 1.4.

Figure 2 shows the prediction of rate of mass loss employing second order kinetics, using inferred equation [7] and the developed equation [6] at 5 ^{o}Cmin^{-1} heating rate. It is clear from the figure that the experimental data were best predicted by the modified equation [6]. The second order predicted values are lower than the experimental reported data points whereas the inferred equation [7] resulted in much higher values. The developed equation according to expression [6] predicted matching values to experimental points.

In experimental results interpretation, rates of mass loss were generated as function of pyrolysis temperature for different heating rates. Figure 3 presents the rate of mass loss against pyrolysis temperature for 3, 5 and 10 ^{o}Cmin^{-1}selected heating rates. It can be seen from Figure 3, that clear maxima are exhibited with pyrolysis temperature for indicated heating rates and the corresponding rates of mass loss.

This behavior was observed for all other studied heating rates. For instance, the rate of mass loss at 3 ^{o}Cmin^{-1} heating rate is found to be 0.133 mgmin^{-1} occurring at 395^{o}C while 0.42 mgmin^{-1} is reported for 10 ^{o}Cmin^{-1} at 425^{o}C. These magnitudes indicated that rate of mass loss per degree

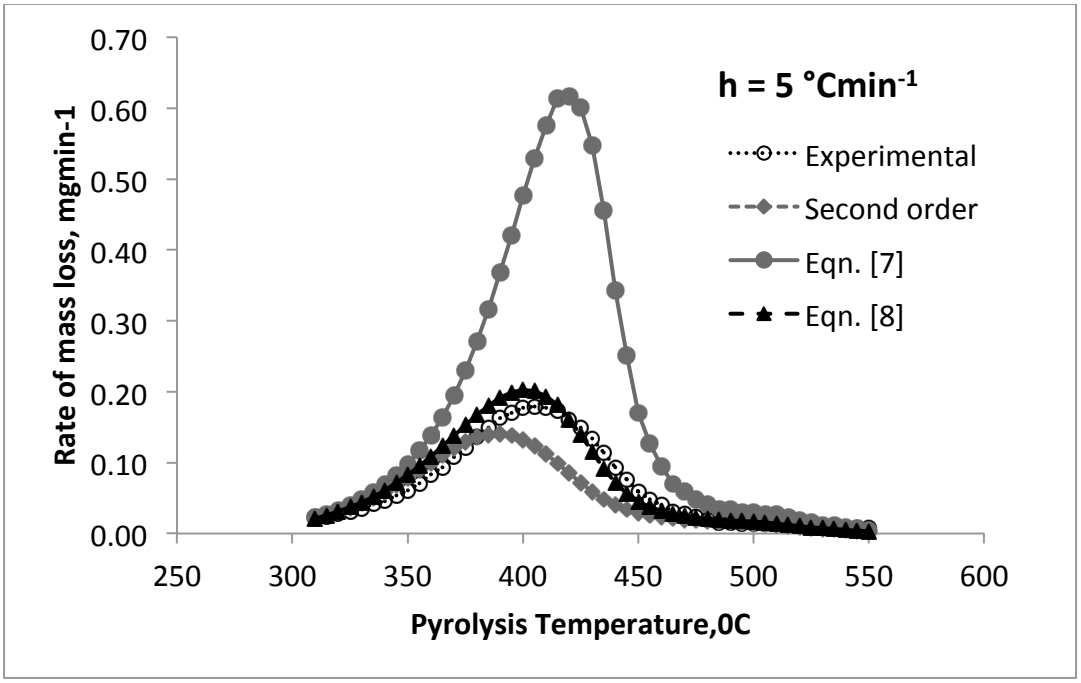

Figure 2: prediction of mass loss rate by different kinetic equation exponent.

centigrade per minute was 0.042 and it is constant in all investigated runs. The only difference was the location of the maximum rate of mass loss with pyrolysis temperature.

Figure 4 depicts the variation of estimated

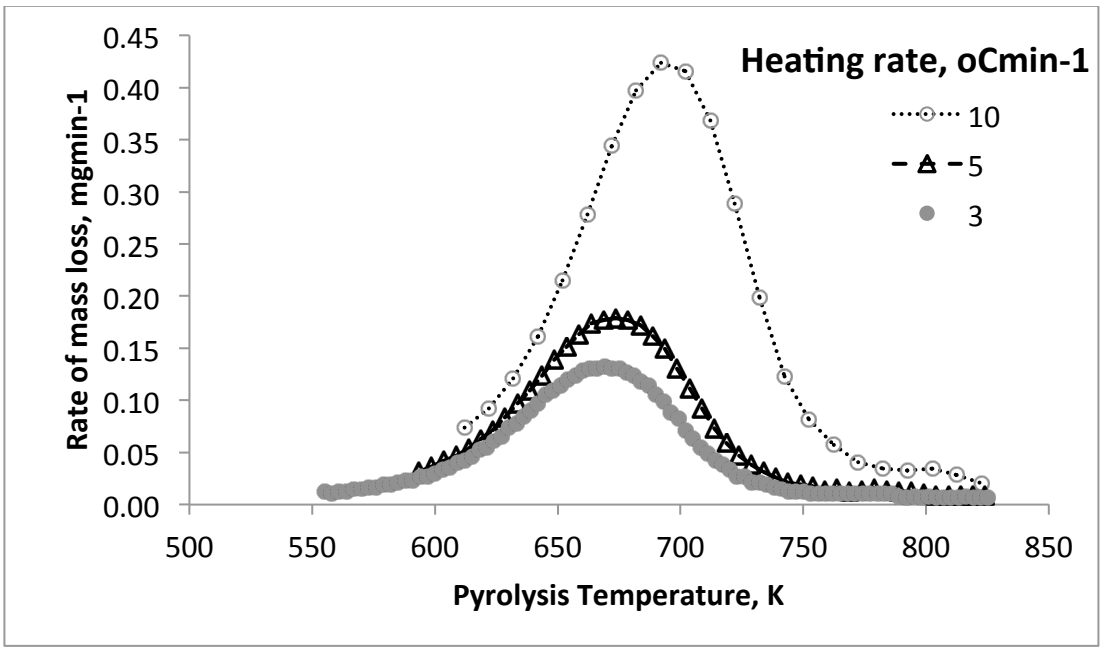

Figure 3: Experimental rate of mass loss against pyrolysis temperature at different heating rates.

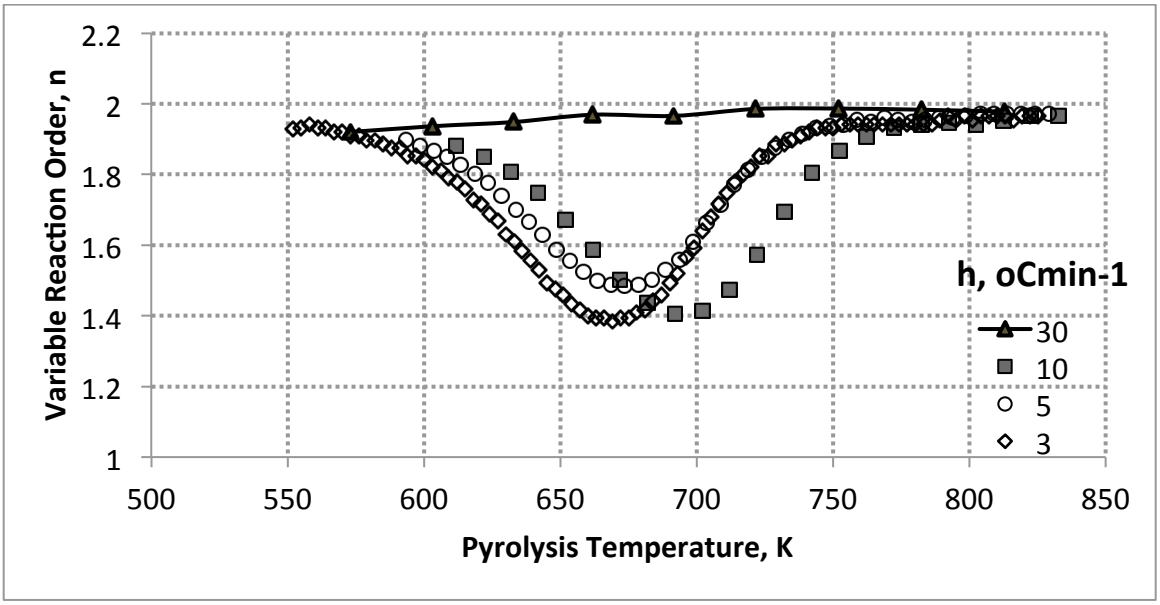

Figure 4: Variation of variable reaction order with pyrolysis temperature and heating rates.

variable reaction order according to equation [7] with pyrolysis temperature for selected 3, 5, 10 and 30 $^{o}Cmin^{-1}$ heating rates. It can be seen from the figure that the variable reaction order passes through a minimum value at 400 to 410 ^{o}C temperature range depending upon heating rate. This minimum magnitude of variable reaction order which lies in the range of 1.3 – 1.4, corresponds to the maximum rate of mass loss at the indicated heating rate. Inspecting the figure further, it can be observed that the reaction order decreases with increasing pyrolysis temperature until maximum rate of mass loss, which corresponds to a minimum value of the variable order.

In addition, in this region of decreasing variable order; higher heating rate produces higher reaction order at same pyrolysis temperature. Lower variable order is observed for higher heating rates with pyrolysis temperature in the region of decreasing rate of mass loss away or to the right of the maximum rate value. It can be also seen from the graph that at the initiation and diminishing rates of mass loss the reaction order values are close to same value.

It was suggested by researchers [19], that reaction order is a firm indicator of reaction mechanism; the shape of Figure 4 supports that belief and further augments the assertion that oil shale reactions are different from normal chemical reactions in that complex parallel, series, and simultaneous reactions are taking place during pyrolysis. The continuous changing values of reaction order with pyrolysis temperature is indicative of changing reaction mechanisms. Changing the reaction order could be a result of types of reactions that were taking place due to instability of the products, or secondary reactions, change of apparent activation energy, effect of varying of pre-exponential factor, which is an implicit function of apparent activation energy in such a complex system.

The estimated activation energy for each heating rate according to the Coats and Redfern procedure was used in conjunction with the developed variable reaction order to estimate the rate of mass loss of sam-

ples obtained from TG data according to the following equation:

$$\frac{dx}{dt} = k_0 exp(-E/RT)(1-x)^{2exp\left(-R\left(\frac{1}{h}\right)dw/dt\right)} \quad [8]$$

As a first step in modeling the rate of mass loss, the variable order is generated according to equation [6] from TGA data for each run. The result of estimating the rate of mass loss by equation [8] for 1 ^{o}Cmin^{-1} heating rate is shown in Figure 5. It should be mentioned here that during curve fitting of data, the calculated frequency factor from the Coats & Redfern procedure did not produce the required fit, and as a result, frequency factor magnitude was modified. The fit of the data was obtained by adjusting frequency factor to higher levels.

It is clear from the figure that introducing variable reaction order in equation [4] to obtain equation [8] improved the prediction of mass loss rate immensely. Figures 5, 6, 7, and 8 are obtained when equation [8] is applied for, 1, 5, 10 and 30 ^{o}Cmin^{-1} heating rates respectively. These figures clearly show that when equation [7] was used in modeling kinetics of different rates of mass loss, a good fit to the experimental data was achieved. The application of the developed equation to different heating rates investigated in this study supports the variable reaction order assumption. It is worth mentioning here that it was not possible to apply the variable reaction order to equation [4] during the step of activation energy determination due to the complexity of mathematics involved. If the variable order is introduced to equation [4] prior to the activation energy determination step, the high non-linearity and the complexity of the mathematical equation makes the whole procedure impossible to proceed.

These figures clearly show that variable reaction order estimated by equation [6] enhances the fit of TGA data compared with a second order kinetic equation. Normally higher heating rate results in more scattering of experimental data due to the

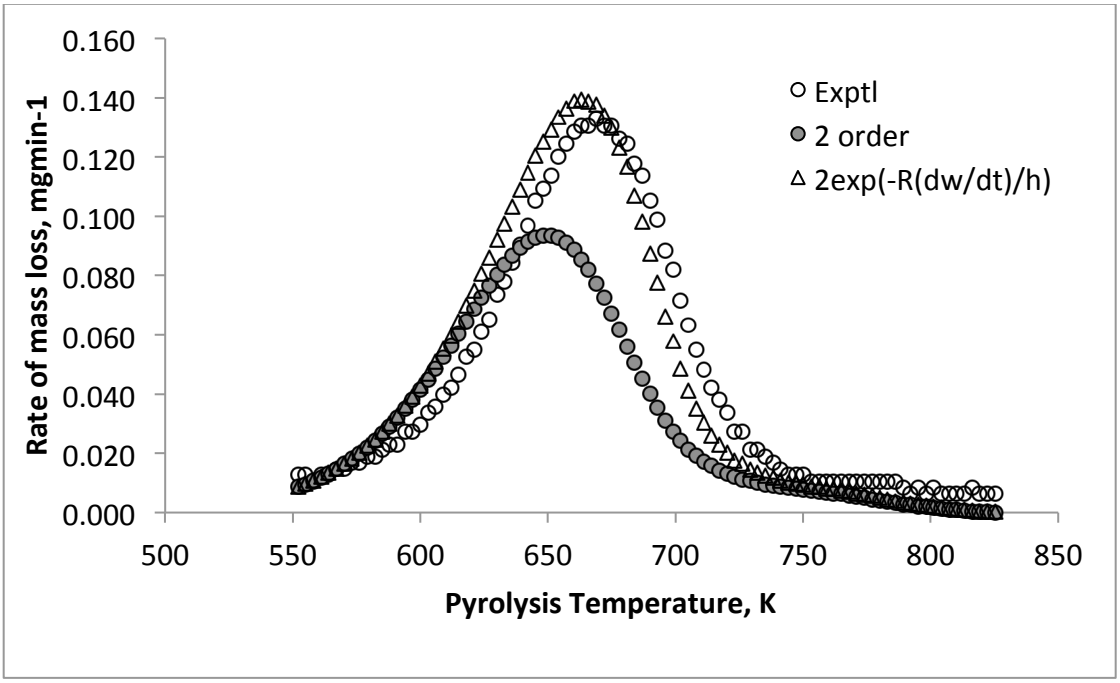

Figure 5: Rate of mass loss against pyrolysis temperature for experimental, second and variable orders at 1^{o}Cmin^{-1} heating rate

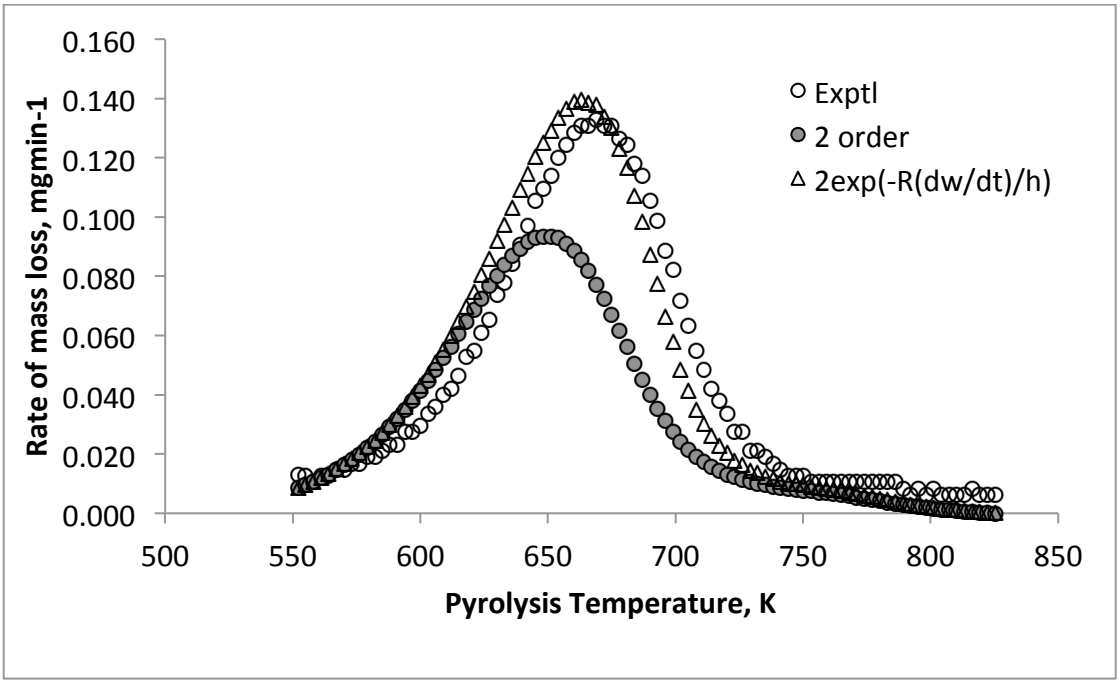

Figure 6: Rate of mass loss against pyrolysis temperature for experimental, second and variable orders at 5°Cmin^{-1} heating rate

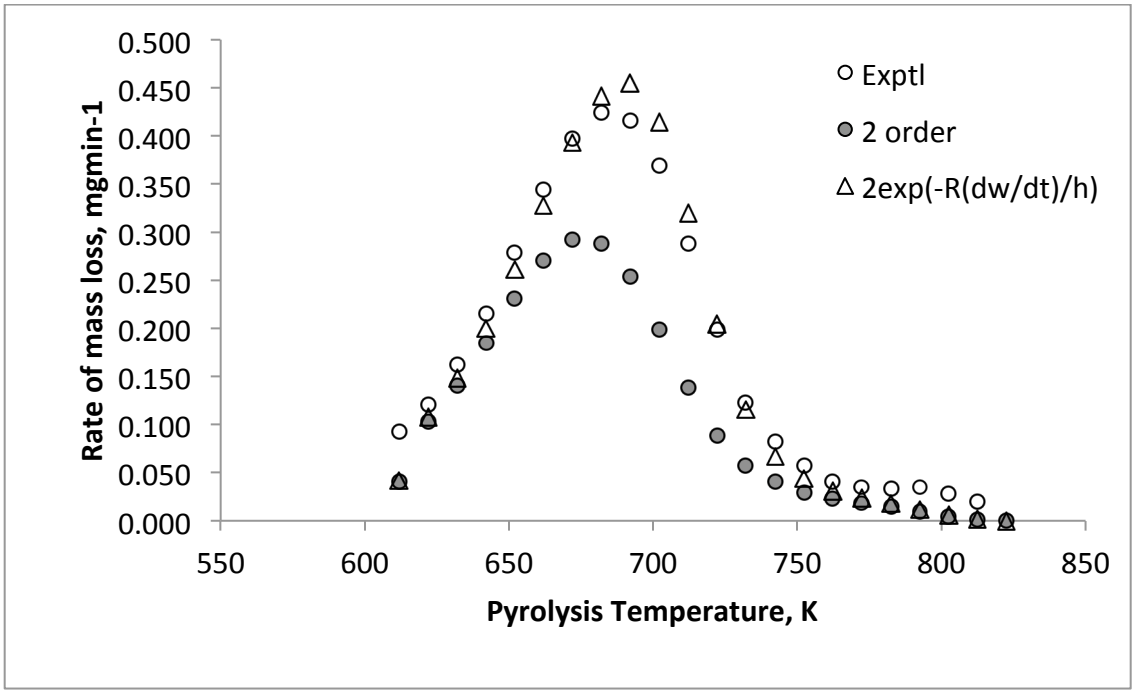

Figure 7: Rate of mass loss against pyrolysis temperature for experimental, second and variable orders at 10 °Cmin^{-1} heating rate

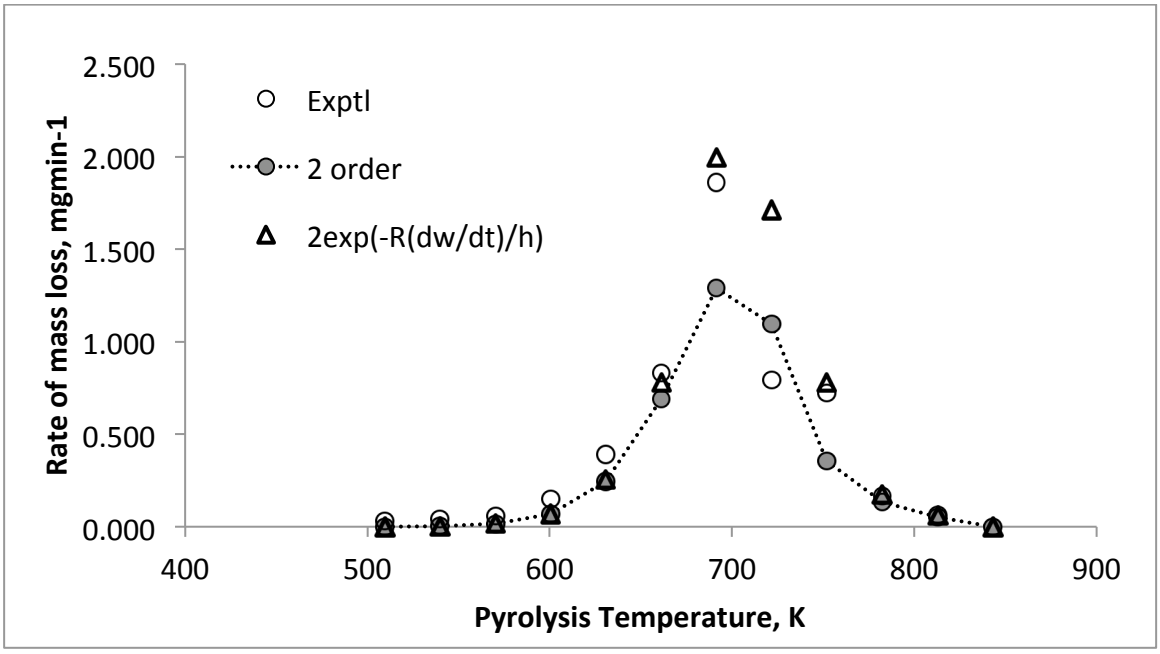

Figure 8: Rate of mass loss against pyrolysis temperature for experimental, second and variable orders at 30 $^{o}Cmin^{-1}$ heating rate

large increase in temperature per unit time; this is clear in Figure 8 where modeling a heating rate of 30 $^{o}Cmin^{-1}$ data produced scattered results, but a good fit was obtained when variable order was used to model the rate of mass loss.

Kerogen modeling

A similar analysis was performed on kerogen samples. The variable order was tested against TGA data for kerogen modeling. The rate of mass loss of kerogen samples was predicted using equation [8] in which the rate of mass loss of kerogen was used in the aforesaid equation. Some of the results have been depicted in Figures 9 and 10. Figure 9 presents a prediction for the rate of mass loss of kerogen at 5$^{o}Cmin^{-1}$ heating rate. The depicted results are the experimental, the second order and the variable model. It can be seen from figure that the variable order improved the fit of the data compared with second order kinetic model.

Similar results are shown in Figure 10, where the rate of kerogen mass loss is plotted against pyrolysis temperature at 3$^{o}Cmin^{-1}$. It can be seen in the figure that the variable order resulted in a better fit compared with the second order equation. These figures 9 and 10 are part of the total results of kerogen modeling using a variable order reaction order. Similar good results were obtained for other heating rates in kerogen modeling.

Conclusions

Rate of mass loss of oil shale is modeled by the standard formula used by majority of workers. The order of reaction is obtained from a plot of reaction order against rate of mass loss. The curve fitting of plotted data resulted in correlating reaction order to rate of mass loss and heating rate in an exponential function. The constants of the obtained equation have been modified slightly to be of the final form:

$$n = 2exp\left(-R\frac{1}{h}(dw/dt)\right)$$

The newly developed variable reaction order is used to model the rate of mass loss of Ellajjun oil shale samples at 1, 3, 5, 10, and 30°$Cmin^{-1}$ heating rates. The kinetic

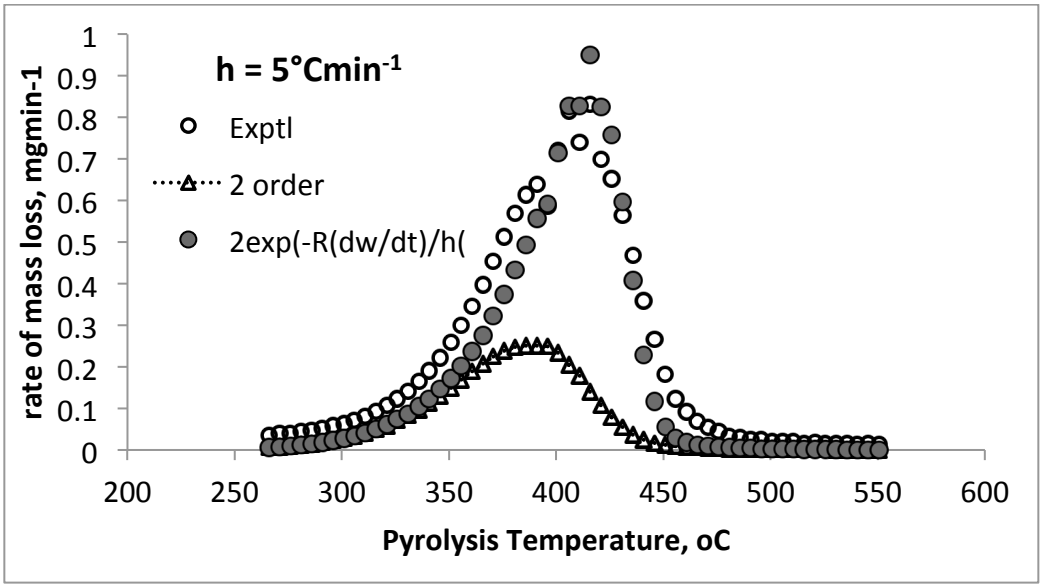

Figure 9: Rate of mass loss against pyrolysis temperature for experimental, second and variable orders at 5 $^{o}Cmin^{-1}$ heating rate for kerogen sample.

modeling of rates of mass loss using variable order is compared with second order kinetics resulting in a more satisfactory results being obtained.

The developed equation was employed to model kerogen pyrolysis and good results were also obtained.

References

1. M. V. Kök and A. G. Iscan, *Oil Shale Kinetics by Differential Methods*, Journal of Thermal Analysis and Calorimetry, Vol. 88 (2007) 3, 657–661.

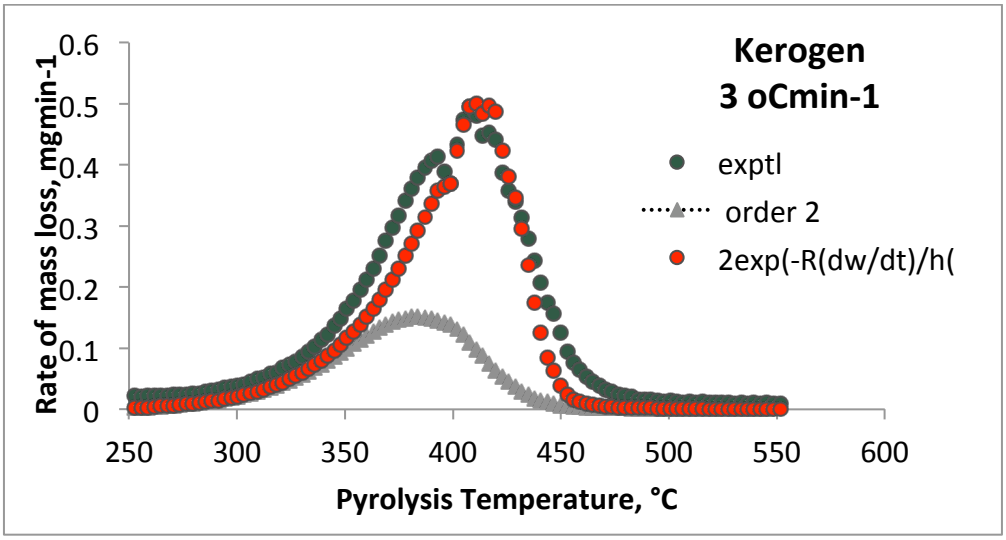

Figure 10: Rate of mass loss against pyrolysis temperature for experimental, second and variable orders at 3 $^{o}Cmin^{-1}$ heating rate for kerogen sample

2. Campbell J.H., Gallegos, G. and Gregg M. *Gas Evolution during Oil Shale Pyrolysis. Kinetic and Stoichiometric Analysis*. 1980, Fuel, 59, 727-732.
3. Bhargava S., Awaja, F., Subasinghe, N.D., *Characterization of Some Australian Oil Shale using Thermal, X-ray and IR techniques*, 2005, Fuel, 84, 707-715.
4. S. Li, C. Yue, *Study of different models for oil shale pyrolysis*, Fuel Processing Technology 85 (2003) 51–61.
5. Djurcic M., Murphy, R.C., Vitorovic D., Biemann K., *Organic acids obtained by alkaline permanganate oxidation of kerogen from the Green River (Colorado) shale*, Geochim Cosmochim Acta, vol 35 (12), 1971, 1201-1207..
6. Young D.K., Yen T.F., *The nature of straight-chain aliphatic structures in green river kerogen*, Geochim Cosmochim Acta, Volume 41, Issue 10, October 1977, 1411-1417.
7. D. S. Thakur and H. E. Nuttall, Ind. Eng. Chem. Res., 26 (1987) 1351.
8. Karabakan and Y. Yurum, *Effect of the mineral matrix in the reactions of shales. Part 2. Oxidation reactions of Turkish Göynük and US Western Reference oil shales*, Fuel, Volume 79, Issue 7, May 2000, Pages 785-792.
9. S. Yagmur and T. Durusoy *Kinetics of the pyrolysis and combustion of göynük oilshale* Journal of Thermal Analysis and Calorimetry, Vol. 86 (2006) 2, 479–482.
10. H. Sütcü, and S. Piskin, *Pyrolysis Kinetics of Oil Shale from Ulukisla, Turkey*,Oil Shale, 2009, Vol. 26, No. 4, pp. 491–499.
11. W. Qing, B. Sun, A. Hu, Baijingeru and S. Li, *Pyrolysis Characteristics of Huadian Oil Shales*, 2007, Oil Shale, Vol. 24(2), 147-157.
12. Jaber J.O., Probert, S.D., *Pyrolysis and Gasification Kinetics of Jordanian Oil Shales*, 1999, Applied Energy, 63(4). 269-286.
13. O.S. Al-Ayed, M. Matouq, Z. Anbar, Adnan Khaleel and Eyad Abu-Nameh, *Oil Shale Pyrolysis Kinetics and Variable Activation Energy Principle*, Applied Energy Journal, 87 , issue 4 (2010) 1269–1272.
14. O.S. Al-Ayed, M. R. Sulieman and Nafi. Yousif. *Kinetic Modeling of liquid Generation from Oil Shale in a Fixed Bed Retort*. 2010, Applied Energy Journal, Vol 87, 2273-2277
15. W. Qing, L. Hongpeng, S. Baizhong and L. Shaohua, *Study on Pyrolysis Characteristics of Huadian Oil Shale with Isoconversional Method*, Oil Shale Journal, Vol. 26(2), 2009, 148-162.
16. S. Vyazovkin, C.A. Wight, *Model-free and model-fitting approaches to kinetic analysis of isothermal and nonisothermal data*, Thermochim. Acta. Vol. 340-341. 1999, 53-68.
17. M.C. Torrente, M.A. Galan, *Kinetics of the thermal decomposition of oil shale from Puertollano (Spain)*, Fuel 80 (2001) 327– 334.
18. J. Šestăk, and G. Berggren, *Study of the Kinetics of the Mechanism of Solid-State Reactions at increasing temperatures*, Thermochim. Acta. Vol. 3, No. 2, 1971, 1-12.
19. Levenspiel O., Chemical Reaction Engineering, 3rd ed., John Wiley & Sons, New York, 1999.
20. Aboulkas, A., El Harfi, K. *Study of the kinetics and mechanisms of thermal decomposition of Moroccan Tarfaya oil shale and its kerogen*, Oil Shale" 2008, Vol 25, No. 4. P. 426–443.
21. D. Skala, H. Kopsch, M., Sokić, H.J., Neumann, 1987. *Thermogravimerically and differential Scanning Calorimetrically Derived Kinetics of Oil Shale Pyrolysis*, Fuel 66 (1987) 1185-1191.
22. Johannes, K. Kruusement and R. Veski, *Evaluation of Oil Potential and Pyrolysis*

Kinetics of Renewable Fuel and Shale Samples by Rock-Eval Analyzer, J. Anal. Appl. Pyrolysis, 79 (2007) 183-190.

23. D. Skala, H. Kopsch, H. Sokić, H.J. Neumann, J.A. Jovanović, *Kinetics and Modeling of Oil Shale Pyrolysis*. Fuel, 69 (1990) 490-496.
24. R.L. Braun, and A.J. Rothman, *Oil Shale Pyrolysis: Kinetics and Mechanism of Oil Production*, Fuel, 54, 1975, 129-131.
25. R.L. Braun A.J., and Rothman. *Oil Shale Pyrolysis: Kinetics and Mechanism of Oil Production*, Fuel, 54 (1975) 129-131.
26. A.W. Coats and J.P. Redfern, *Kinetic Parameter from Thermogravimetric Data*, Nature, Vol 201, 1964,68-69.
27. M. Á. Olivella, and F. X. C. De Las Heras. *Evaluation of Linear Kinetic Methods from Pyrolysis Data of Spanish Oil Shales and Coals*, Oil Shale. 2008, Vol. 25, No. 2. p. 227-245